FEEDBACK STABILISED BIFURCATION TAILORING APPLIED TO AIRCRAFT MODELS

G.A.Charles , M.H.Lowenberg , X.F.Wang , D.P.Stoten , M.Di Bernardo
Faculty of Engineering, University of Bristol, UK

Keywords: *nonlinear dynamics, bifurcation diagram, feedback control*

Abstract

Bifurcation tailoring is a technique that uses bifurcation analysis to create feedforward control signals in order to change the bifurcation diagram of a system to some given desired one. In it's original feedforward alone implementation bifurcation tailoring had no guarantee of stability or uniqueness of the new bifurcation diagram. The addition of a feedback control loop, in this case an adaptive reference model strategy known as the Minimal Control Synthesis (MCS), solves these problems. This paper covers the background theory to bifurcation tailoring and gives as examples the application of the technique to 2nd order highly manoeuvrable nonlinear flight dynamics.

1 Introduction

The use of bifurcation theory is becoming widespread in the analysis of nonlinear dynamics and control strategies. References [29, 27] provide a good introduction to the area of nonlinear dynamics. Bifurcation theory provides the natural environment in which to study nonlinear aircraft dynamics in terms of state versus parameter behaviour [28]. Particularly with the advent of better aircraft modelling and the availability of cheap computing power the use of numerical applications has allowed dynamicists to investigate beyond the linearised trim solutions and delve into the complex mechanics of flight. Bifurcation analysis has been applied in many situations to flight dynamics, for example: in the sense of producing bifurcation diagrams for the aircraft under the variation of one or two parameters (e.g. elevator) [31, 20, 18, 13, 11]; or, stability and boundary of attraction analysis of equilibrium values [6, 23, 14]. Bifurcation control in aerospace applications has mainly been restricted to individual points in the state phase space [22], or around a region of a Hopf point [1]. Reference [28] contains a good review of nonlinear analysis in the aerospace industry.

Bifurcation tailoring is a novel technique that allows the aircraft dynamicist to control the aircraft throughout its flight regime by altering the system's entire bifurcation diagram. This is achieved by appropriately varying other system parameters (e.g. control surfaces or thrust vector angle) in addition to the bifurcation parameter (say, elevator or stick position). In this sense bifurcation tailoring is a considerable departure from the idea of stabilising small areas of the bifurcation diagram. In bifurcation tailoring the aim is to use the available parameters to change and stabilise the whole bifurcation diagram, using fully the modern numerical tools available. Bifurcation tailoring has been successfully applied to flight models in an *open loop* sense, i.e. in an entirely scheduled feedforward control guise, where the feedforward signal was created in an off-line continuation program [19]. However, in this feedforward only configuration the stability or uniqueness of solution cannot be guaranteed. Reference [21] proposed using the bifurcation tailoring to schedule the gains in a feedback controller throughout the flight regime: an improvement over the standard approach of interpolating between several calculated gain values at individual points in the flight regime.

The problems associated with the feedforward scheduled bifurcation tailoring as described above can be overcome by the use of a feedback control strategy in addition to the feedforward schedule [3]. There is a rich area of research concerned with the control of nonlinear systems and bifurcations. These include using normal forms [15, 16], harmonic balances [9], or wash out filters [30, 2]. References [5, 4] are good reviews of the area of bifurcation and chaos control. In this paper we have selected a control strategy using an adaptive model reference controller known as the Minimal Control Synthesis (MCS) [24, 25]. This has already been applied in many engineering situations including the control of chaotic systems [26]. MCS will ensure the stability and uniqueness *throughout* the desired bifurcation diagram, *and* provide the control designer with an opportunity to control the dynamic response of the aircraft through the eigenvalues of the reference model chosen in the MCS controller.

This paper aims to demonstrate the method of application of the bifurcation tailoring technique to flight dynamics. Background is first given in section 2. In this paper we have chosen to present in detail the work carried out on the simpler 2nd order flight dynamics. This still constitutes a complex nonlinear model, with comprehensive aerodynamic information. The purpose is to demonstrate the principles of bifurcation tailoring and the additional feedback control, and although recent work has shown the technique to be successful when used on higher order systems, this is easier to perform with the 2nd order model. Bifurcation tailoring applied to the second order aircraft model in order to produce an arbitrary bifurcation diagram is presented in section 3. Section 4 contains some further results from bifurcation tailoring applied to the second order flight dynamics model, using the pilot stick position as a bifurcation parameter. Conclusions from these results are drawn in section 5.

2 Background

2.1 Bifurcation Tailoring

Consider a continuous time dynamical system described by

$$\dot{\mathbf{x}} = \mathbf{f}(\mathbf{x}, p, \mathbf{q}) \tag{1}$$

where $\mathbf{x} \in \Re^n$ is the state of the system, $p \in \Re$ we assume to be a slow varying system parameter (bifurcation parameter) and $\mathbf{q} \in \Re^m$ is the vector of all the other system parameters. The *bifurcation tailoring* problem is to design a control law $\mathbf{q}$ such that the controlled system has the desired dynamical behaviour as the parameter p varies from p_a to p_b.

Consider the bifurcation tailoring problem where the desired objective for the controlled system is to exhibit a branch of equilibria such that, as the parameter p is varied,

$$\mathbf{x}_{Id} = \mathbf{g}(p) \tag{2}$$

where

$$\mathbf{x} = \begin{bmatrix} \mathbf{x}_I \\ \mathbf{x}_{II} \end{bmatrix}, \mathbf{x}_I = \begin{bmatrix} x_1 \\ \vdots \\ x_m \end{bmatrix}, \mathbf{x}_{II} = \begin{bmatrix} x_{m+1} \\ \vdots \\ x_n \end{bmatrix}$$

Defining the auxiliary vector as:

$$\mathbf{z} = \begin{bmatrix} \mathbf{x}_{II} \\ \mathbf{q} \end{bmatrix} \tag{3}$$

we have that for any given $p \in [p_a, p_b]$ the system must satisfy the equation:

$$\mathbf{f}(\mathbf{g}(p), \mathbf{x}_{II}, p, \mathbf{q}) \equiv \tilde{\mathbf{f}}(\mathbf{g}(p), p, \mathbf{z}) = 0 \tag{4}$$

The Implicit Function Theorem [10] states that if the Jacobian of $\mathbf{f}$ w.r.t. $\mathbf{z}$ is invertible, then (4) implicitly defines $\mathbf{z}$ as a function of p i.e.

$$\mathbf{z} = \mathbf{z}_d(p) = \begin{bmatrix} \mathbf{x}_{IId}(p) \\ \mathbf{q}_d(p) \end{bmatrix} \tag{5}$$

which means that

$$\mathbf{x} = \begin{bmatrix} \mathbf{x}_{Id} \\ \mathbf{x}_{IId} \end{bmatrix} \tag{6}$$

is an equilibrium point of the feedforward open loop system

$$\dot{\mathbf{x}} = \mathbf{f}(\mathbf{x}, p, \mathbf{q}_d(p)) \tag{7}$$

Hence the desired equilibria defined by (2) is a set of equilibria in the feedforward system (7). Figure 1 shows the block diagram for this technique.

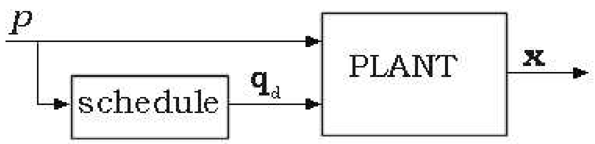

Fig. 1 Block diagram for the scheduled feedforward control system ("open loop" bifurcation tailoring)

2.2 Constructing the feedforward schedule

Typically it is not a viable option to find the feedforward schedule analytically using eqn (4). Thus, the schedule is created numerically to obtain a set of tabulated data. This process can be carried out using a bifurcation continuation program such as AUTO [7]. This software would usually be used to solve for the state, $\mathbf{x}$, whilst varying one parameter, p. We can invert the process to solve eqn (4), i.e. solve for $\mathbf{z}(p)$ given the function $\mathbf{g}(p)$ and varying one parameter, p.

2.3 Feedforward Bifurcation Tailoring Limitations

1. The AUTO continuation program requires a *full, accurate* mathematical model to create the correct $\mathbf{q}_d$.

2. Undesired equilibria may be created in addition to the desired equilibria.

3. The stability of the equilibria is not assured.

4. The equilibrium $\mathbf{x}_d$ may not exist for some value of $p = p_e$, in which case there is no solution for $\mathbf{q}_d(p_e)$.

Problems 2 and 3 suggest that some sort of feedback mechanism would be beneficial. This would also overcome some inaccuracies in the mathematical model used to create the feedforward signal (problem 1). Problem 4 is a problem for *any* controller using the same control input, $\mathbf{q}$, and may for example, be seen as control actuator saturation. The technique of bifurcation tailoring can, in fact, bring these limitations to the attention of the control designer very early in the design process.

2.4 Feedback Stabilisation

For the bifurcation tailoring applications in this paper an adaptive model reference controller known as Minimal Control Synthesis (MCS) was used. This is an appropriate solution as the controller automatically tunes the gains as the plant changes throughout the range of p. The control input is given by:

$$\mathbf{q}(t) = \mathbf{q}_d(t) + \Delta\mathbf{q}(t) \tag{8}$$

where $\mathbf{q}_d(t)$ is the schedule (derived from tabulated data from AUTO) and $\Delta\mathbf{q}(t)$ is the stabilisation control from the MCS equations:

$$\begin{aligned}
\Delta\mathbf{q}(t) &= K(t)\mathbf{x}(t) + K_R(t)\mathbf{x}_d(t) \\
K(t) &= \alpha_M \int \mathbf{y}_e(\tau)\mathbf{x}^T(\tau)d\tau + \beta_M \mathbf{y}_e(t)\mathbf{x}^T(t) \\
K_R(t) &= \alpha_M \int \mathbf{y}_e(\tau)\mathbf{x}_d^T(\tau)d\tau + \beta_M \mathbf{y}_e(t)\mathbf{x}_d^T(t) \\
\mathbf{y}_e(t) &= C_e\mathbf{x}_e(t) = C_e(\mathbf{x}_m - \mathbf{x})
\end{aligned}$$

where $\alpha_M \in \Re$, $\beta_M \in \Re$ and $C_e \in \Re^{m,n}$ are constants, and where the linear reference model is given by the standard linear state space model:

$$\dot{\mathbf{x}}_m = A_m\mathbf{x}_m + B_m\mathbf{x}_d \tag{9}$$

The MCS controller is so useful in this application as not only can the stability of the desired solution be assured [24, 25], but the dynamic response of the aircraft can be controlled in the region around the desired solution through the linear reference model [17]. If we set $B_m = -A_m$ we ensure that $x_m = x_d$ at equilibrium. Bearing this

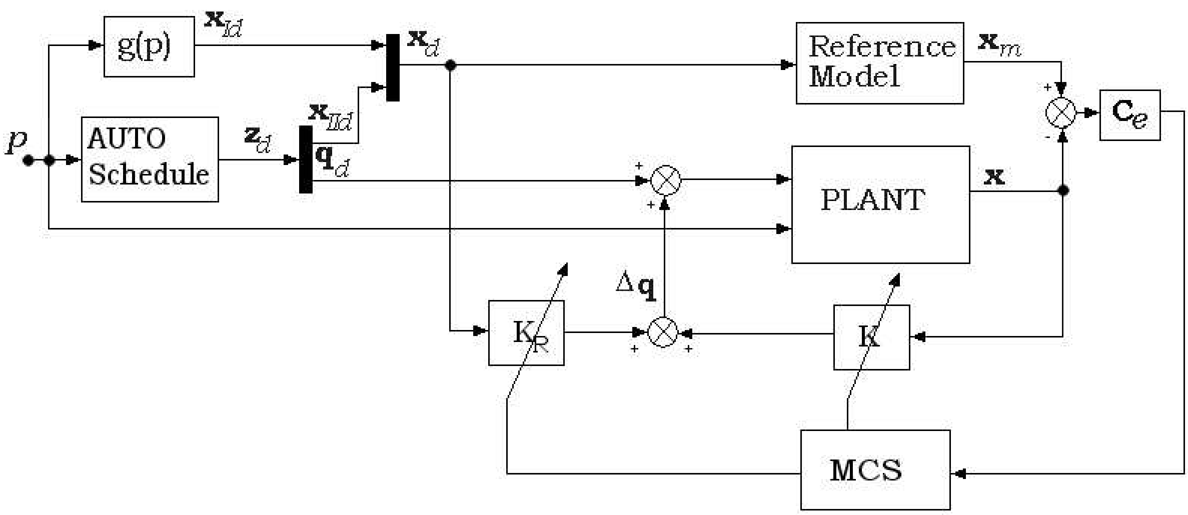

Fig. 2 Block diagram for the MCS feedback stabilised feedforward scheduled system

in mind, inspection of the MCS equations reveals that, providing the eigenvalues of A_m have negative real parts, at equilibrium $x = x_d$. The MCS controller will ensure that the system tracks the reference model in the region around the equilibrium value, allowing the control designer to place the eigenvalues of the system throughout the range of p. Figure 2 shows the block diagram for the feedforward MCS feedback stabilised control.

3 Bifurcation Tailoring Applied to the Second Order Model

3.1 Second Order HHIRM Aircraft Model

The aircraft model used in this paper is a highly manoeuvrable non-linear model called the Hypothetical High angle of Incidence Research Model (HHIRM) [12], provided by QinetiQ. For this report it is used in a second order form that describes the fast longitudinal dynamics of the aircraft [8]:

$$\begin{cases} \dot{\alpha} = q + \frac{\bar{q}S(C_z \cos\alpha - C_x \sin\alpha)}{mV_T} + \frac{g\cos(\alpha)}{V_T} \\ \dot{q} = \frac{\bar{q}ScC_m}{I_y} \end{cases} \tag{10}$$

where α is the angle of attack, q is the pitch rate, $C_z = f_z(\alpha, \delta_{el}, \delta_{tp})$ is the coefficient of the force in the z direction, $C_x = f_x(\alpha, \delta_{el}, \delta_{tp})$ is the coefficient of the thrust in the x direction, $C_m = f_m(\alpha, \delta_{el}, \delta_{tp})$ is coefficient of the pitching moment, δ_{el} is the elevator angle, δ_{tp} is the thrust vectoring angle in the pitching sense, $\bar{q}$ is the dynamic pressure (assumed constant due to constant velocity and height), other constants are: S, the total wing area; m, the mass; V_T, the airspeed; g, the acceleration due to gravity; c, the chord length; I_y, the moment of inertia about the pitching axis. We can write (10) more generally as

$$\begin{bmatrix} \dot{\alpha} \\ \dot{q} \end{bmatrix} = \mathbf{f}(\alpha, q, \delta_{el}, \delta_{tp}) \tag{11}$$

We are going to take δ_{el} as the bifurcation (or continuation) parameter. Hence we use δ_{tp} as a further control parameter to allow feedforward control (figure 3). Since there is only one control input ($\mathbf{q} = \delta_{tp}$), i.e. $m = 1$, there can only be one pre-defined desired state in $\mathbf{x}_I$ in equation (2).

Figure 4 shows the bifurcation surface for the HHIRM model. The initial bifurcation analysis is crucial, so as to be able to define possible desired bifurcation diagrams and understand what the limits of control saturation may be. Figure 5 shows the limits of the surface, i.e. bifurcation diagrams created at the limits of δ_{tp}. Nominally the limits are $\delta_{tp} = \pm 90°$. Although this is entirely unrealistic, this is good practice to ensure

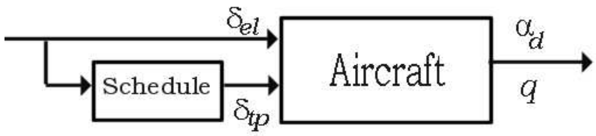

Fig. 3 Block diagram for the feedforward scheduled (only) HHIRM model

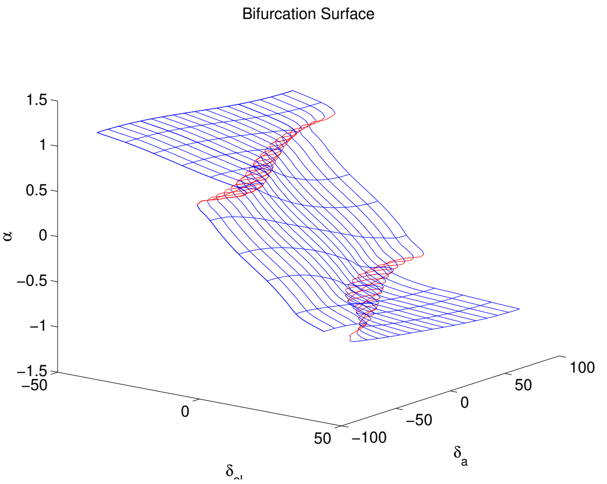

Fig. 4 Bifurcation surface for the 2nd order HHIRM model (created using AUTO). Blue lines=stable, Red lines=unstable

all branches within the physically limited parameter space are investigated. Knowing the bifurcation surface will also help aid the understanding of the closed loop control dynamics.

Figure 6 shows the original bifurcation plot for α vs δ_{el} for the HHIRM model (with $\delta_{tp} = 0$). Figure 7 shows the HHIRM simulation response under the same conditions ($\delta_{tp} = 0$). When a gradual decrease in the elevator angle from zero to $-25°$ was applied to the HHIRM model simulation the angle of attack gradually increased up to $-19.5°$ ($\alpha = 0.59$ rad $= 33.8°$) where there was a catastrophic 'drop' from the edge of the fold in figure 6 up to the higher α branch.

3.2 Feedforward scheduling

Figure 8 shows the user-defined desired bifurcation diagram for α. This arbitrary shape was chosen because of its simplicity and for its smooth

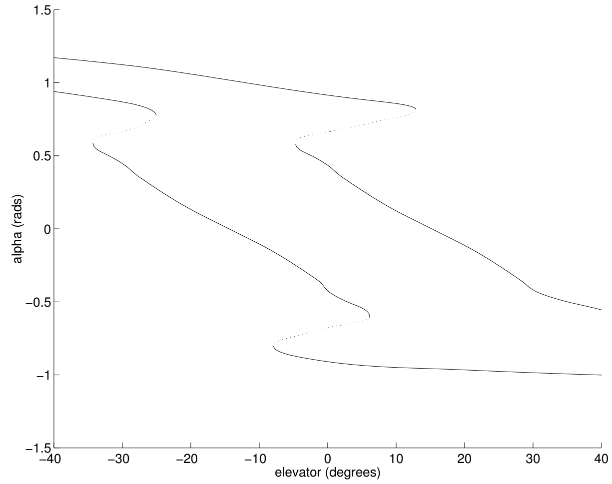

Fig. 5 Bifurcation diagrams plotted at the limits of δ_{tp}. Solid lines = stable, dotted lines = unstable

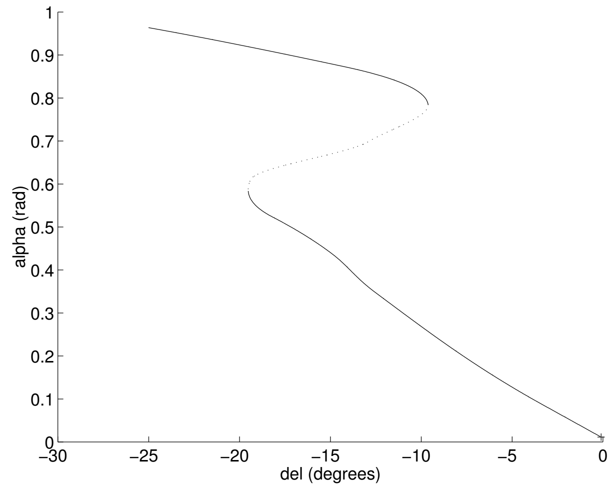

Fig. 6 Bifurcation plot for the 2nd order HHIRM model with $\delta_{tp} = 0$ (created using AUTO). Solid lines=stable, dotted lines=unstable.

qualities, hence it can easily be applied to a bifurcation continuation program or numerical simulation. Figure 9 shows the *ideal* schedule for δ_{tp} created via AUTO, that when applied to the HHIRM model ensured that the desired equilibria existed.

The bifurcation diagram created using AUTO for the 2nd order HHIRM model using the feedforward schedule alone is shown in figure 10. The desired equilibria have been created in the system but there are also unwanted equilibria so-

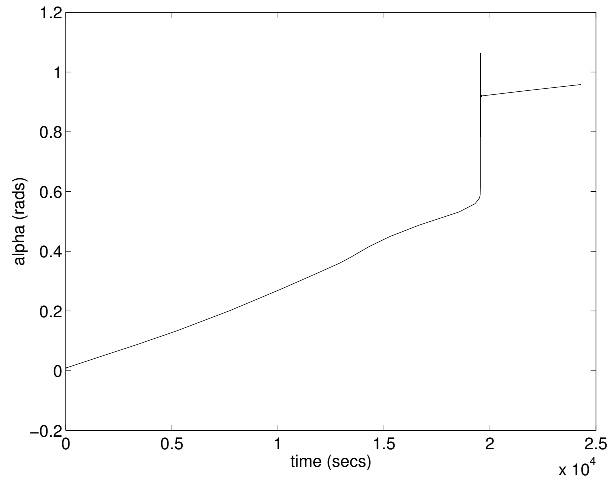

Fig. 7 Simulation of the HHIRM model with $\delta_{tp} = 0$ and $\dot{\delta_{el}} = -0.001°/s$

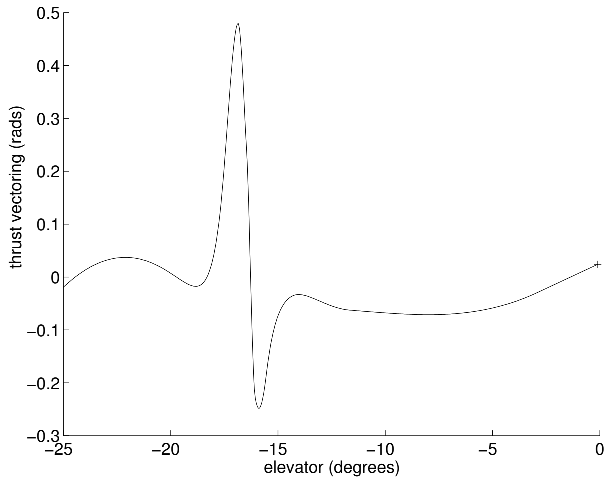

Fig. 9 The *ideal* schedule that when applied to the HHIRM model results in the desired equilibria (figure 8)

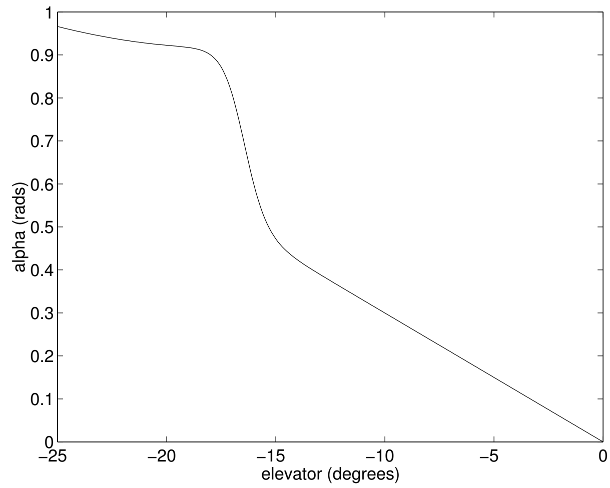

Fig. 8 Desired bifurcation function for the 2nd order HHIRM model

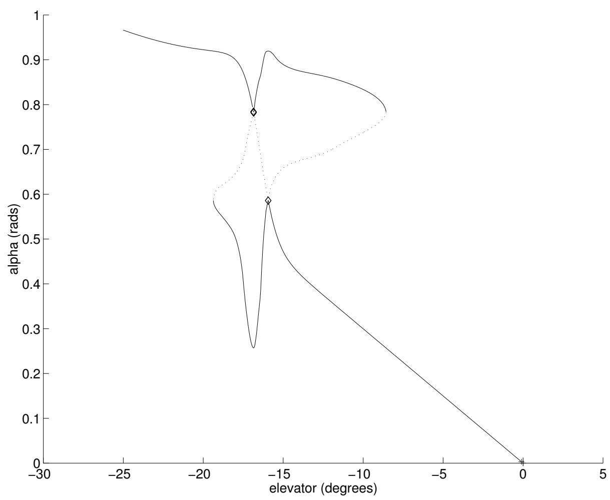

Fig. 10 The bifurcation diagram created using the *ideal* feedforward schedule (figure 9).

lutions and regions of instability. The additional unwanted equilibria can be understood by looking at the bifurcation surface shown in figure 4. A bifurcation diagram is typically made with all but one of the parameters fixed. Looking at the surface, the original bifurcation diagram (figure 6) would therefore be simply a straight 'slice' through the surface with $\delta_{tp} = 0$. The addition of the feedforward schedule makes the 'slice' through the surface follow a curved path, as δ_{tp} follows the schedule. This will result in the desired equilibria as plotted against δ_{el} but as there may be more than one equilibrium point at each $(\delta_{el}, \delta_{tp})$ point along the schedule, other undesired equilibria may be picked out. In the case of the 2nd order HHIRM surface we have unwanted equilibria in the folded region where there are three equilibria points for each $(\delta_{el}, \delta_{tp})$ point.

Figure 11 shows the simulation response when the feedforward schedule alone is applied to the 2nd order HHIRM model. The elevator is moved slowly ($\dot{\delta_{el}} = -0.001°/s$) in order to verify the bifurcation diagram created using AUTO.

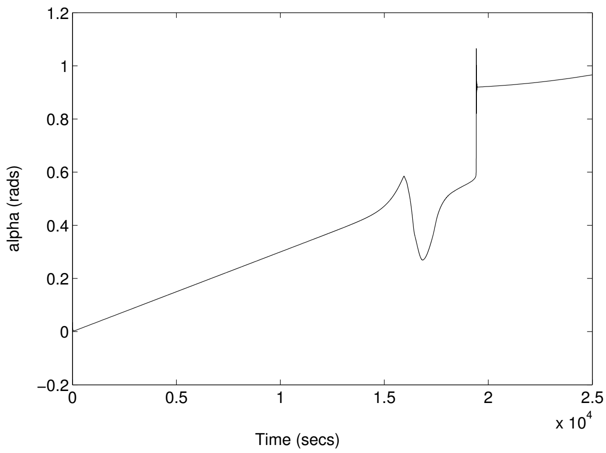

Fig. 11 The simulation response for the feedforward scheduled (alone) 2nd order HHIRM model. $\dot{\delta_{el}} = -0.001°/s$

They match well, with the simulation following the lower stable equilibria as expected when the elevator angle is decreased from 0 to –25°.

3.3 Feedback Stabilisation

Figure 12 shows the block diagram for the feedback stabilised HHIRM model. The feedback stabilisation was provided by the MCS algorithm (see section 2.4) in order to stabilise the desired α vs δ_{el} equilibria in the $\delta_{el} = -16°$ to $\delta_{el} = -17°$ region (see figures 10 and 11). Figure 13 shows the response of the HHIRM model after the addition of the feedback stabilisation. The small control effort required by the MCS controller can be seen in figure 14.

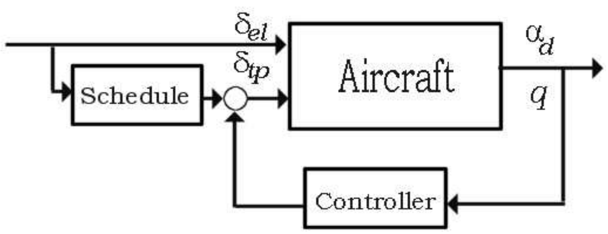

Fig. 12 Block diagram showing the feedforward scheduled HHIRM model plus feedback stabilisation

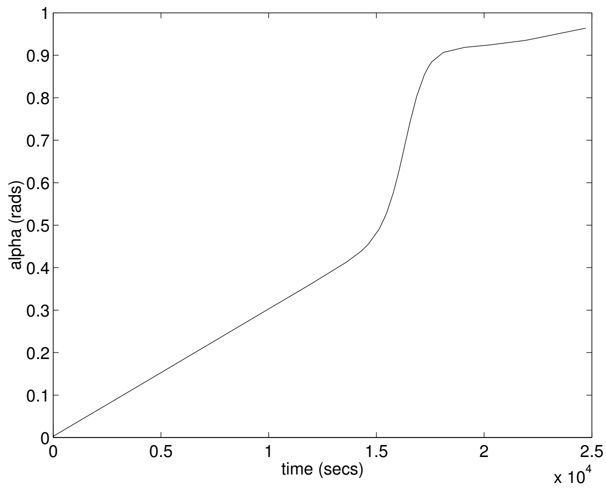

Fig. 13 Simulation of the HHIRM with feedforward scheduling and MCS feedback stabilisation. $\dot{\delta_{el}} = -0.001°/s$

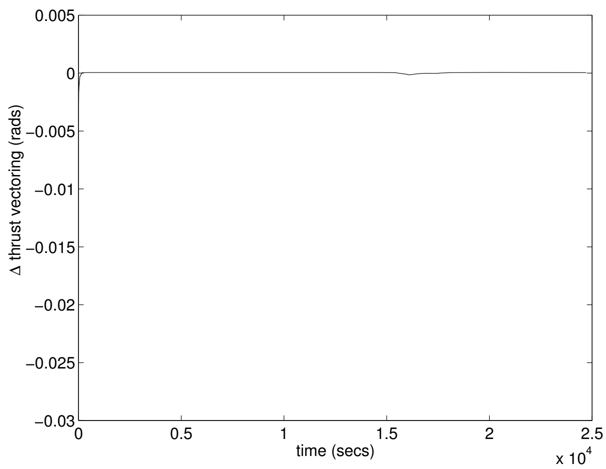

Fig. 14 Simulation of the HHIRM with feedforward scheduling and MCS feedback stabilisation. $\dot{\delta_{el}} = -0.001°/s$

The entire range of elevator is now stable and produces a unique (desired) equilibrium. As δ_{el} reduces (the aircraft moves in a nose up sense), the response is now to move in a smooth path from the 'lower' branch to the 'upper' branch, instead of the abrupt change in α seen in figures 7 and 11. Moreover, it can be noted that the reference model in the MCS algorithm (equation 9) allows the control designer to control some aspects of the response of the aircraft in the neighbourhood of the equilibria. In effect the eigenvalues of the controlled system are set via the reference model over the desired bifurcation diagram equilibria.

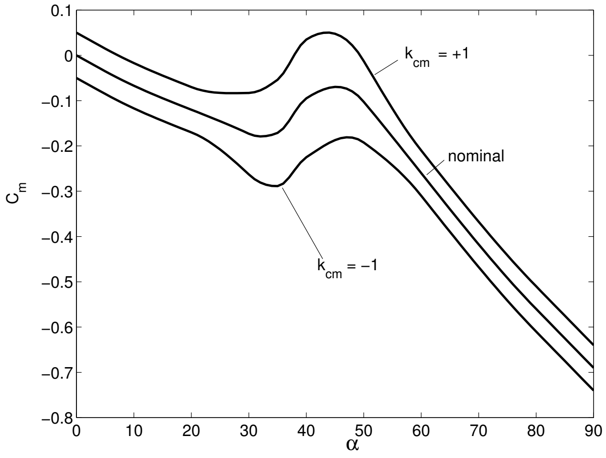

Fig. 15 The variation in C_m, the pitching moment coefficient, due to variations in k_{cm}, the pitching moment coefficient tolerance.

The purpose of the MCS stabilisation is also to ensure the correct bifurcation branch with the addition of unknowns in the system. This could be in the form of noise on the output signals, but in this case model variation was included by changing the variation in the pitching moment coefficient over the range of α. Figure 15 shows the effect of varying the tolerance term, k_{cm}, has on the pitching moment. For these tests $k_{cm} = 0.1$. Figure 16 shows that the desired response is still achieved under these conditions. Figure 17 shows that the MCS controller has to put in more effort in order to counter the changes in the plant.

4 Bifurcation Tailoring using two parameters

The previous sections have dealt with demonstrating the concept of bifurcation tailoring by applying it to second order nonlinear flight dynamics. So far we have dealt with tailoring one particular state by changing one additional parameter as the bifurcation parameter varies, but

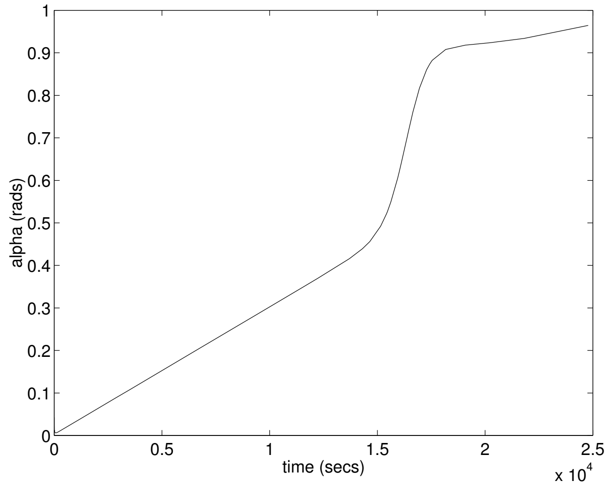

Fig. 16 Simulation of the HHIRM (including variations from the nominal model) with feedforward scheduling and MCS feedback stabilisation. $\dot{\delta_{el}} = -0.001°/s$

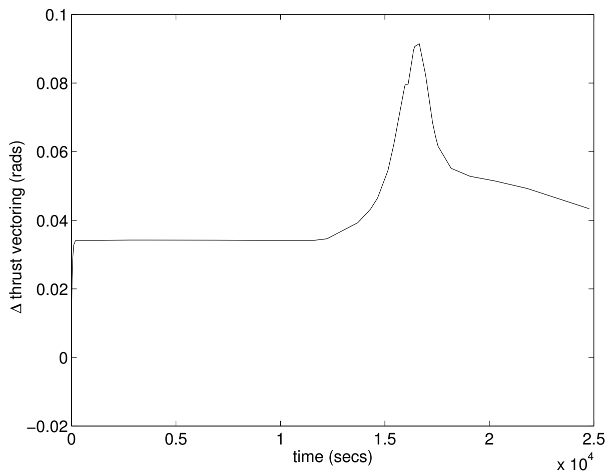

Fig. 17 Simulation of the HHIRM (including variations from the nominal model) with feedforward scheduling and MCS feedback stabilisation. $\dot{\delta_{el}} = -0.001°/s$

it is apparent that the technique should be able to be applied to more than one state. Looking at the aircraft dynamics from a more practical point of view, the pilot in a control augmented aircraft does not have a direct link between the stick and, say, elevator. That means that we may not want a particular bifurcation diagram with respect to elevator, but with respect to stick position (SP). This corresponds to a manoeuvre demand system and allows us to have two additional parameters available for bifurcation tailoring. The theory laid out in section 2.1 shows that we can therefore create schedules to achieve a desired bifurcation diagram for two states. Effectively we are allowing the parameters to 'roam' over the surface to follow the desired bifurcation equilibria as the stick position varies.

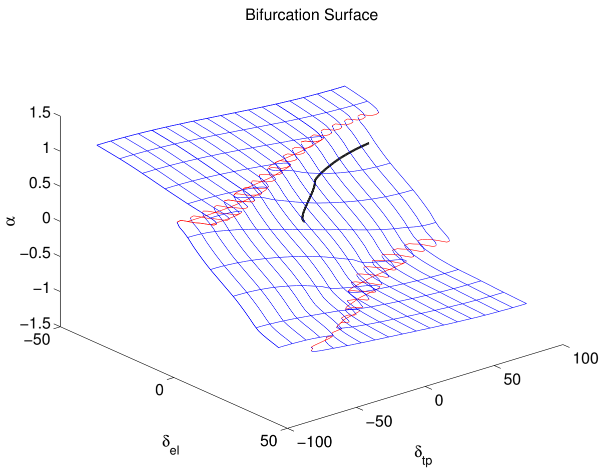

Fig. 18 Schedule created for δ_{el} and δ_{tp} using AUTO plotted over the α bifurcation surface. Blue are stable equilibria, Red are unstable. The schedule is shown in black.

The process is the same as for the previous sections, but now $x_d \in \Re^2$, and hence we will create a schedule, $q_d \in \Re^2$. In this instance, we select a linear relationship between the stick position and both α and q. Figures 18 and 19 show the schedules created for δ_{el} and δ_{tp} plotted over the bifurcation surfaces for α and q. As before the equilibria traced out by following the schedule are all embedded in the original system. As a result of following these schedules, if the bifurcation diagram for the state is plotted against the arbitrary bifurcation parameter, stick position (figures 20 and 21), we achieve the desired straight line bifurcation diagrams.

In practice the task of defining two bifurcation diagrams to be picked out of two different surfaces at the same values of δ_{el} and δ_{tp} without reaching the control limits (edges of the surface)

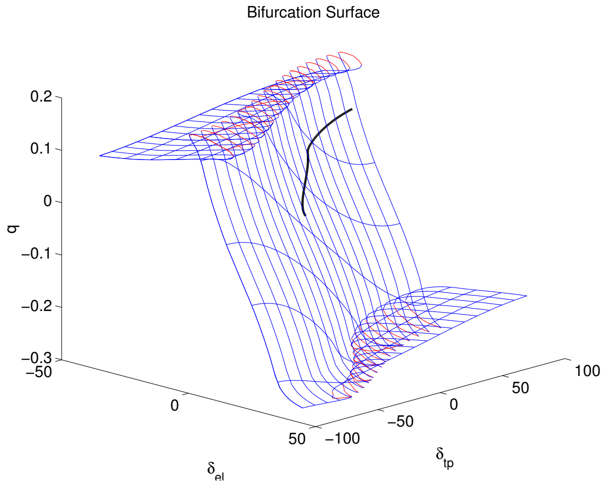

Fig. 19 Schedule created for δ_{el} and δ_{tp} using AUTO plotted over the q bifurcation surface. Blue are stable equilibria, Red are unstable. The schedule is shown in black.

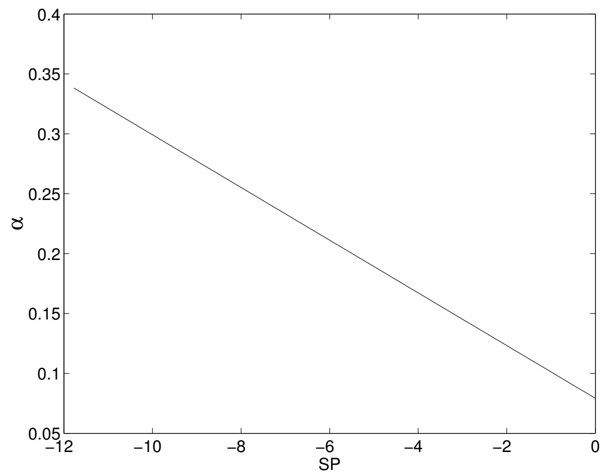

Fig. 20 Bifurcation diagram for α with respect to the stick position

proved to be difficult. The use of the original bifurcation surfaces was essential at this point to be able to select possible desired bifurcation diagrams. There was little difficulty in finding the schedules using AUTO once this was achieved. These problems could be addressed using optimisation routines to minimise the deviation from the desired bifurcation diagrams when creating the schedules, while allowing AUTO some flexibility to continue through difficult regions of the

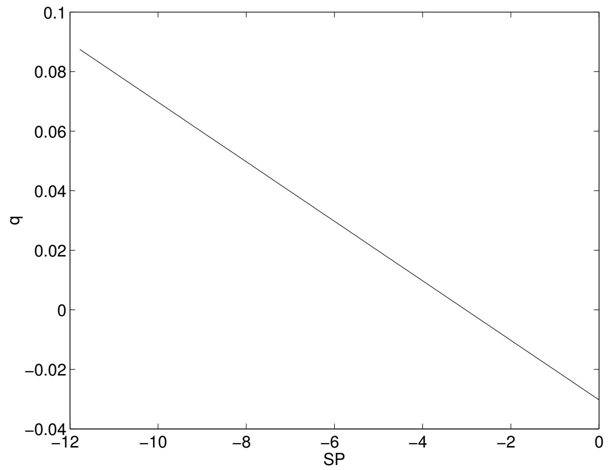

Fig. 21 Bifurcation diagram for q with respect to the stick position

bifurcation surfaces.

5 Conclusions

Bifurcation analysis and nonlinear control are being used more often in practical aerospace applications. The novel method for controlling nonlinear systems given by the bifurcation tailoring technique allows the bifurcation diagram of the controlled system to be changed to a given entirely new one. This process has been demonstrated to work successfully in tailoring the angle of attack bifurcation diagram with respect to elevator for a second order highly manoeuvrable flight dynamics model. This was achieved by appropriately varying the thrust vectoring as the elevator varies to achieve the desired bifurcation diagram with respect to elevator. The addition of the adaptive feedback controller in the guise of the MCS completes the strategy in terms of stability and uniqueness of solution and gives the designer the chance to control the response of the system around the desired equilibria by selecting the reference model in the MCS equations. Therefore we have removed the fold and unstable region in the original system bifurcation diagram and replaced it with a smooth unique set of stable equilibria.

Although we have applied the bifurcation tailoring process to a low order nonlinear system to create arbitrarily shaped bifurcation diagrams, the power of the technique is apparent. So long as the equilibria exist in the original system, we can create a feedforward schedule and apply a feedback control loop to achieve a unique stable set of desired equilibria.

Furthermore we have demonstrated that by using the two available control parameters in the second order flight dynamics model (elevator and thrust vectoring), we can apply bifurcation tailoring to both angle of attack and pitch rate, with respect to a new bifurcation parameter, stick position. On going research is being carried out into extending these ideas, and furthering the work carried out on higher order models.

6 Acknowledgments

The authors would like to thank the EPSRC (grant number GR/M97923) for their support. The support of QinetiQ in providing the HHIRM flight model is also gratefully acknowledged.

References

[1] Abed E and Lee H. Nonlinear stabilisation of high angle-of-attack flight dynamics using bifurcation control. No TR 90-32. American Control Conference, 1990.

[2] Abed E, Wang H, and Tesi A. *The Control handbook*, chapter 57.6, pp 951–966. IEEE, 1996.

[3] Charles G, di Bernardo M, Lowenberg M, Stoten D, and Wang X. Bifurcation tailoring of equilibria: a feedback control approach. *Latin American Applied Research*, Vol. 31, No 3, pp 199–210, 2001.

[4] Chen G and Dong X. From chaos to order - perspectives and methodologies in controlling chaotic nonlinear dynamical systems. *International Journal of Bifurcation and Chaos*, Vol. 3, No 6, pp 1363–1409, 1993.

[5] Chen G, Moiola J, and Wang H. Bifurcation control: theories, methods and applications. *International Journal of Bifurcation and Chaos*, , No 10, pp 511–548, 2000.

[6] Cochran J and Ho C.-S. Stability of aircraft

motion in critical cases. *Journal of Guidance*, Vol. 6, No 4, pp 272–279, 1983.

[7] Doedel E and Wang X. Auto94: Software for continuation and bifurcation problems in ordinary differential equations. Technical Report CRPC-95-2, California Institute of Technology, 1995.

[8] Etkin B and Reid L. *Dynamics of Flight: Stability and Control*. John Wiley and Sons, Inc, 1996.

[9] Genesio R, Tesi A, Wang H, and Abed E. Control of period doubling bifurcations using harmonic balance. No 0191-2216/93. IEEE Conference on Decicion and Control, 1993.

[10] Glendinning P. *Stability, instability and chaos: an introduction to the theory of nonlinear differential equations*. Cambridge University Press, 1994.

[11] Goman M, Khramtsovsky A, and Shapiro M. Aerodynamics modeling and dynamics simulation at high angles of attack. Technical report, TsAGI, 2001.

[12] Goman M, Khramtsovsky A, and Usoltev S. High incidence aerodynamics model for hypothetical aircraft. Technical Report 15/5dra, TsAGI, 1995.

[13] Guicheteau P. Non-linear flight dynamics. *AGARD lecture series 191*, , No 191, 1993.

[14] Jahnke C and Chen G. Nonlinear stability analysis of aircraft steady states. No AIAA-953449. AIAA, 1995.

[15] Kang W. Bifurcation and normal form of nonlinear control systems, part 1. *SIAM Journal of Control Optim.*, Vol. 36, No 1, pp 193–212, 1998.

[16] Kang W. Bifurcation and normal form of nonlinear control systems, part 2. *SIAM Journal of Control Optim.*, Vol. 36, No 1, pp 213–232, 1998.

[17] Landau Y. *Adaptive Control: The Model Reference Approach*. Marcel Dekker, Inc, 1979.

[18] Lowenberg M. Bifurcation analysis of multiple-attractor flight dynamics. *Philosophical Transactions of the Royal Society of London*, Vol. 356, pp 2297–2319, 1998.

[19] Lowenberg M. Development of control strategies to modify spin behaviour. No AIAA-98-4267. AIAA Atmospheric Flight Mechanics Conference, 1998.

[20] Lowenberg M and Champneys A. Shil'nikov homoclinic dynamics and the escape from roll autorotation in an f-4 model. *Phil. Trans. Royal Society London*, , No 356, pp 2241–2256, 1998.

[21] Lowenberg M and Richardson T. The continuation design framework for nonlinear aircraft control. No AIAA-2001-4100. AIAA, 2001.

[22] Pinsky M and Essary B. Resonance control of aircraft instabilities by smooth and continuous feedback. *Journal of Guidance, Control and Dynamics*, Vol. 18, No 6, pp 1298–1304, 1995.

[23] Shrivastava P and Stengel R. Stability boundness for aircraft with unstable lateral-directional dynamics and control saturation. *Journal of Guidance*, Vol. 12, No 1, pp 62–70, 1989.

[24] Stoten D and Benchoubane H. Empirical studies of an mrac algorithm with minimal control synthesis. *International Journal of Control*, , No 51, pp 823–849, 1990.

[25] Stoten D and Benchoubane H. Robustness of a minimal control synthesis algorithm. *International Journal of Control*, , No 51, pp 851–861, 1990.

[26] Stoten D and Di Bernardo M. Application of the minimal control synthesis algorithm to the control and synchronization of chaotic systems. *International Journal of Control*, Vol. 65, No 6, pp 925–938, 1996.

[27] Strogatz S. *Nonlinear Dynamics and Chaos: with Applications to Physics, Biology, Chemistry and Engineering*. Addison-Wesley, 1994.

[28] Thompson J and (eds.) F. M. Nonlinear flight dynamcis of high-performance aircraft. *Philosophical Transcriptions of the Royal Society of London*, Vol. 356, pp 2163–2333, 1998.

[29] Thompson J and Stewart H. A tutorial glossary of geometrical dynamics. *Internation Journal of Bifurcation and Chaos*, Vol. 3, No 2, pp 223–239, 1993.

[30] Wang H and Abed E. Bifurcation control of a chaotic system. *Automatica*, Vol. 31, No 9, pp 1213–1226, 1995.

[31] Young J, Schy A, and Johnson K. Prediction of jump phenomena in aircraft maneuvers including nonlinear aerodynamic effects. *Journal of Guidance and Control*, Vol. 1, No 1, pp 26–31, 1978.